Pergamon

PII: S0277-5387(97)00065-X

*Polyhedron* Vol. 16, No. 19, pp. 3421-3427, 1997

0277-5387/97 $17.00+0.00

# Characterization of the non-stoichiometry in lanthanum oxyfluoride by FT-IR absorption, Raman scattering, X-ray powder diffraction and thermal analysis

Jorma Hölsä,[a] Eija Säilynoja,[a] Hanna Rahiala[a]* and Jussi Valkonen[b]

[a] University of Turku, Department of Chemistry, FIN-20014 Turku, Finland

[b] University of Jyväskylä, Department of Chemistry, P.O. Box 35, FIN-40351 Jyväskylä, Finland

(Received 20 September 1996; accepted 4 February 1997)

**Abstract**—The FT-IR absorption, FT-Raman scattering, X-ray powder diffraction (XPD), and thermogravimetry were used to explore the non-stoichiometry in LaOF. The TGA-DTA analyses between 30 and 1500°C showed that the $LaO_{1-x}F_{1+2x}$ phases yielded the stoichiometric LaOF as an intermediate product. The temperature of formation of the LaOF and $La_2O_3$ increased with increasing excess of fluoride.

The room temperature XPD data in $6.5 \leqslant 2\theta \leqslant 121°$ range were analyzed by the Rietveld profile refinement method and subsequently by the bond valence calculations. All $LaO_{1-x}F_{1+2x}$ phases possess the tetragonal PbFCl-type structure (space group: $P4/nmm$; $Z = 2$) while the stoichiometric LaOF has the hexagonal SmSI-type structure (space group: $R\bar{3}m$; $Z = 6$). The unit cell parameters $a$ and $c$ as well as the global instability index (GII) values increased with increasing excess fluoride. The GII value for each $LaO_{1-x}F_{1+2x}$ exceeded the limit (*ca* 0.2) for a possible breakdown of the tetragonal structure indicating the inherent instability of these phases.

The room temperature FTIR and FT-Raman spectra between 100 and 500 $cm^{-1}$ and 50 and 1000 $cm^{-1}$, respectively, were investigated using the factor group analysis to get more information of the local structure in LaOF. All four IR modes ($2A_{2u}+2E_u$) for the both forms and five of the six Raman modes ($3A_{1g}+3E_g$ and $A_{1g}+2B_{1g}+3E_g$) for the hexagonal and the tetragonal form, respectively, were observed. The Raman spectra of the tetragonal LaOCl and all $LaO_{1-x}F_{1+2x}$ were found remarkably similar. © 1997 Elsevier Science Ltd

*Keywords*: lanthanum oxyfluoride; non-stoichiometry; X-ray powder diffraction; Rietveld refinement; bond valence; Raman scattering; thermoanalysis.

A careful analysis of many inorganic solids reveals that the stoichiometric ratios frequently assume non-integral values. In addition, the compounds usually exhibit a more or less wide range of composition. The ionic compounds tend more often to show non-stoichiometry than the covalent ones since the introduction of ions in excess requires less energy than breaking bonds [1]. However, the non-stoichiometric compounds are frequently of potential use to industry because their electronic, magnetic, optical, and mechanical properties can be modified by changing the composition of the compound.

The X-ray and neutron diffraction are the most frequently used methods to study the crystal structure but these methods usually yield only the *average* structure which omits the precise structural information [2]. It is hence rather difficult to determine the exact structure of the non-stoichiometric compounds. A technique sensitive to the *local* structure is needed. The plausible candidates include the spectroscopic methods, e.g. the IR absorption and Raman scattering techniques. The luminescence spectroscopy may, however, be the most sensitive technique to probe the local structure involving the study of the emission spectra of an impurity voluntarily introduced to the lattice [3]. The use of this technique is limited by the choice of the suitable luminescent probe for each compound to be studied.

* Author to whom correspondence should be addressed.

Various structures have been reported for the ionic rare earth oxyfluorides (LnOF) in the literature. The stoichiometric Ln oxyfluorides belong to the hexagonal crystal system [4]. At high temperatures, the existence of a cubic phase has been indicated [5] as well as of a monoclinic phase for the heavier Ln oxyfluorides [6]. However, the Ln oxyfluorides are also known to exhibit non-stoichiometry with the formation of phases with excess fluoride, $LnO_{1-x}F_{1+2x}$ [7]. Some of the phases in this system have been assigned to different crystal systems, e.g. compositions $LaO_{0.65}F_{1.70}$ and $SmO_{0.70}F_{1.60}$ with the tetragonal [8] and orthorhombic [9] structures, respectively.

Since the information concerning other than structural properties of the Ln oxyfluorides are sometimes as confused (and confusing) [10] as the structural information available, we have in the present investigation carried out the *far*-FTIR absorption, FT-Raman scattering, X-ray powder diffraction (XPD), and simultaneous TGA-DTA studies of the LaOF system. The experimental data were analyzed by the factor group analysis (IR and Raman), and the Rietveld profile refinement (XPD) methods [11]. The structural data were subsequently treated according to the bond valence method [12] in order to find out the relative stabilities of the different lanthanum oxyfluoride phases.

## EXPERIMENTAL

### *Sample preparation*

According to the literature data, the Ln oxyfluorides can be prepared by using several different techniques such as the hydrolysis of $LnF_3$ at 500–900°C [7], heating of the $Ln_2O_3$-$LnF_3$ mixture at 900–1200°C [13], heating of the $Ln_2O_3$-$NH_4F$ mixture [14], and, in general, by thermal decomposition of fluorine containing compounds as Ln fluorocarbonates [15].

In the present study, the lanthanum oxyfluorides were prepared by the solid state reaction between the high-purity (99.99%) $La_2O_3$ and ammonium fluoride at 1050°C for 1.5 h in static ambient atmosphere. The initial $NH_4F/La_2O_3$ ratios were selected between 2.00 and 2.75 but the final composition of the samples was verified later by thermal analysis. The $LaO_{1-x}F_{1+2x}$ phases were doped with a small amount (1 mol%) of $Eu^{3+}$ for the eventual luminescence measurements.

### *Thermal analysis*

The fluoride content and thermal decomposition of the $LaO_{1-x}F_{1+2x}$ phases were studied by using the simultaneous TGA-DTA technique with a SDT 2960 (TA-Instruments) apparatus. The *ca* 10 mg samples were heated in $Al_2O_3$ crucibles from 30 to 1500°C with a heating rate of 5° $min^{-1}$ in air with a flow rate of 100 $cm^3$ $min^{-1}$. Anhydrous $Al_2O_3$ was used as the DTA reference material.

The straightforward calculations based on the TGA curves indicated that the $x$ value in $LaO_{1-x}F_{1+2x}$ changes from 0 to 0.3, which is far below the initial values aimed at with the $NH_4F/La_2O_3$ ratios used in the preparation of these phases.

### *Optical measurements*

The FTIR absorption investigations were carried out at room temperature between 100 and 500 $cm^{-1}$ with a Mattson Galaxy series FTIR 4060 spectrometer. Standard polyethylene technique was used for the sample preparation.

The room temperature FT-Raman scattering spectra were measured with a Bruker FRA 106 FT-Raman accessory between 50 and 1000 $cm^{-1}$. The YAG : Nd laser was used at the wavelength of 1064 nm. The resolution of both the FTIR and FT-Raman set-up was 4 $cm^{-1}$.

### *X-ray powder diffraction measurements*

The X-ray powder diffraction patterns of the lanthanum oxyfluoride samples were measured with a Enraf-Nonius PDS120 X-ray powder diffractometer (Cu-$K_{\alpha_1}$ radiation, $\lambda = 1.5406$ Å) equipped with INEL CPS120 position sensitive detector. The measurements were carried out at room temperature between 6.5 and 121.6° in $2\theta$. Silicon powder (NBS standard 640b) was used as an external standard. The angular resolution of the apparatus was better than 0.018°.

## RESULTS AND DISCUSSION

### *Thermal stability*

The aim of the thermogravimetric measurements was two-fold : first, they were carried out to investigate the precise composition of the non-stoichiometric $LaO_{1-x}F_{1+2x}$ phases. These results have already been described above. Secondly, the thermal stability of the $LaO_{1-x}F_{1+2x}$ phases and, especially the intermediate products were of interest since it has been proposed that a cubic LaOF phase—corresponding to the ideal fluorite structure—may be obtained at high temperatures [5].

The experimental results (Fig. 1) reveal indeed that a stoichiometric LaOF phase is obtained irrespective of the composition of the initial $LaO_{1-x}F_{1+2x}$ phase. The temperature of appearance of the LaOF phase increases with increasing excess fluoride from 875 up to 995°C. The end product, $La_2O_3$, is formed at 1425°C for the non-stoichiometric phases and at a considerably lower temperature, 1370°C, for the stoichiometric LaOF phase.

In the present study, no rhombohedral to cubic phase transformation could be observed at around 494°C reported earlier [16]. This may be due to the

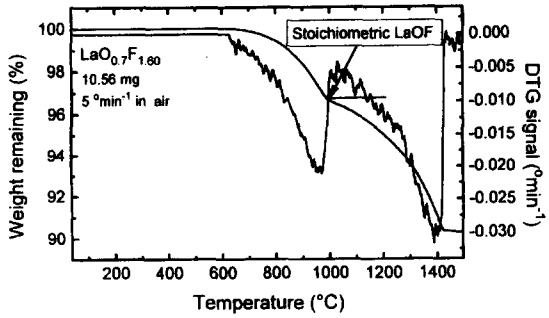


Fig. 1. Thermal decomposition of the non-stoichiometric tetragonal $LaO_{0.70}F_{1.60}$ phase.

limited sensitivity of the apparatus because of a very weak DTA signal caused by the phase transformation. It has also been pointed out that no transition to the cubic phase occurs if the starting phase was a non-stoichiometric tetragonal NdOF [5].

*Structure refinement*

The XPD data were analyzed with the Rietveld profile refinement method [11] by using the DBWS-9006PC program [17]. The Rietveld method is based on minimizing the residual $S_y$ equal to the sum of the square of the difference between the observed and calculated intensity for every data point in the diffraction pattern. The Rietveld analyses were performed with the data between 20 and 120° in $2\theta$ (Fig. 2).

The unit cell, atomic position, isotropic temperature, Gaussian profile form and background parameters were all refined but not always simultaneously. The parameter refinement scheme has been described in detail elsewhere [18]. The Gaussian profile function was corrected for asymmetry for all reflections with $2\theta$ less than 100°. The refinement for the stoichiometric LaOF was carried out according to the hexagonal crystal system while both the tetragonal and orthorhombic systems were used for the non-stoichiometric $LaO_{1-x}F_{1+2x}$ ($0.05 \leqslant x \leqslant 0.3$) phases.

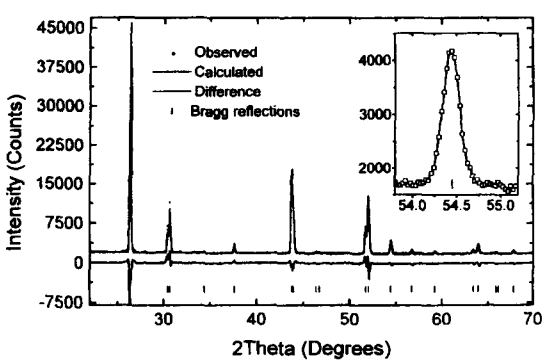


Fig. 2. The observed (scatter), calculated (solid line) and difference (lower) X-ray powder diffraction patterns for $LaO_{0.70}F_{1.60}$ at room temperature ($\lambda$ = 1.5406 Å). The insert depicts the (022) reflection area indicating no splitting and thus no decrease in crystal symmetry from tetragonal to orthorhombic.

The treatment of the non-stoichiometry in $LaO_{1-x}F_{1+2x}$ was based on the assumption that the $F^-$ ions share the $O^{2-}$ site in the tetragonal form of LaOF; space group: $P4/nmm$; no. 129 ($Z = 2$). This is rather difficult to prove experimentally since the X-ray scattering factors for the $F^-$ and $O^{2-}$ ions are very similar and, in practice, the two ions are indistinguishable. The interstitial positions occupied by the excess $F^-$ ions were not considered since there was not found any spectroscopic evidence as to the existence of these site (*cf.* below).

The least-squares calculations were carried out until a constant $R_{wp}$ value was obtained in the refinement between the entire observed and calculated powder diffraction pattern. The $R_{wp}$ values used as a figure of merit of the refinement varied between 5.5 and 9.2% (Table 1) and are satisfactory for such a complicated non-stoichiometric system. One of the most probable reasons for the deviations is the significant overlap of the Bragg reflections in the spectra. Some discrepancy may be also due to the preferred orientation effect since the structures, especially of the tetragonal phase, consist of layers which results in the macroscopic texture of the samples. No further attempts to correct for the preferred orientation were carried out since most of the models used at the moment to account for this effect cannot be considered sufficient. Moreover, the experimental and calculated intensities of reflections at low $2\theta$ values showed no pronounced deviations. The lowest $R_{wp}$ value was obtained for the stoichiometric LaOF phase. The $R_{wp}$ values for the tetragonal and orthorhombic refinements were practically the same, but the latter ones were never lower than the former.

The unit cell parameters $a = 4.0534(6)$ and $c = 20.1961(5)$ Å (space group: $R\bar{3}m$; $Z = 6$) obtained for the hexagonal LaOF are more accurate than, but not significantly different from, the literature values ($a = 4.051$ and $c = 20.121$ Å [7]). The cell parameters for the tetragonal $LaO_{1-x}F_{1+2x}$ phases (Fig. 3) grow slightly as the parameter $x$ increases. The refinement according to the orthorhombic system gave quite similar results to the tetragonal one. The $a$ and $b$ parameters differed only slightly, at the most a few hundreds of Å, and the $R_{wp}$ values were almost identical. It was thus concluded that it was not possible to observe the lowering in symmetry from tetragonal to orthorhombic by the X-ray powder diffraction. Moreover, from the reflection profiles (*cf.* the insert of Fig. 2), there was no evidence found for a real decrease in the crystal symmetry, and thus the results for the orthorhombic system are not presented here.

According to the Rietveld refinements, the structures of both the hexagonal and tetragonal LaOF possess the typical Ln oxycompound structure with distinct alternating layers of the complex cation $(LaO)_n^{n+}$ and the fluoride anions. The difference

Table 1. The unit cell, atom positional, isotropic temperature parameter and $R_{wp}$ values for the $LaO_{1-x}F_{1+2x}$ ($0 \leqslant x \leqslant 0.3$) phases

| Host | $a$ (Å) | $c$ (Å) | $z_{La}$ | $z_F$ | $z_O$ | $B_{La}$ | $B_F$ | $B_O$ | $R_{wp}$ (%) |
|---|---|---|---|---|---|---|---|---|---|
| LaOF[a] | 4.0534(4) | 20.1961(10) | 0.24249(1) | 0.37068(6) | 0.11902(7) | 0.34426 | 0.00560 | 0.40145 | 5.5 |
| $LaO_{0.95}F_{1.10}$ | 4.0850(4) | 5.8320(7) | 0.27592(4) | — | — | 0.20117 | 0.94037 | 0.30822 | 7.5/8.1 |
| $LaO_{0.91}F_{1.18}$ | 4.0906(2) | 5.8386(4) | 0.27991(3) | — | — | 0.29723 | 0.80654 | 0.12877 | 7.8/7.2 |
| $LaO_{0.89}F_{1.22}$ | 4.0942(2) | 5.8423(3) | 0.28057(3) | — | — | 0.19775 | 0.94037 | 0.30822 | 7.4/7.4 |
| $LaO_{0.85}F_{1.30}$ | 4.0927(1) | 5.8386(2) | 0.27887(3) | — | — | 0.19775 | 0.94037 | 0.30822 | 6.2/9.2 |
| $LaO_{0.83}F_{1.34}$ | 4.1202(2) | 5.8765(4) | 0.27998(4) | — | — | 0.25454 | 0.89188 | 0.07618 | 8.7 |
| $LaO_{0.72}F_{1.56}$ | 4.1089(1) | 5.8593(3) | 0.27520(4) | — | — | 0.24595 | 0.94261 | 0.50000 | 8.1 |
| $LaO_{0.70}F_{1.60}$ | 4.1120(1) | 5.8599(3) | 0.27255(4) | — | — | 0.30337 | 0.96510 | 0.71703 | 8.3 |

[a] Hexagonal crystal system.

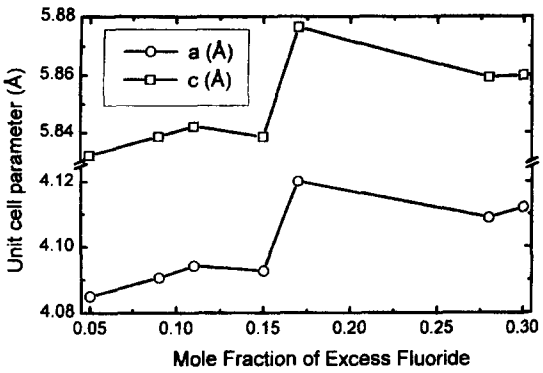


Fig. 3. Evolution of the unit cell parameters in the $LaO_{1-x}F_{1+2x}$ series. The estimated standard deviations of the parameter values are smaller than the symbol height used in the figure.

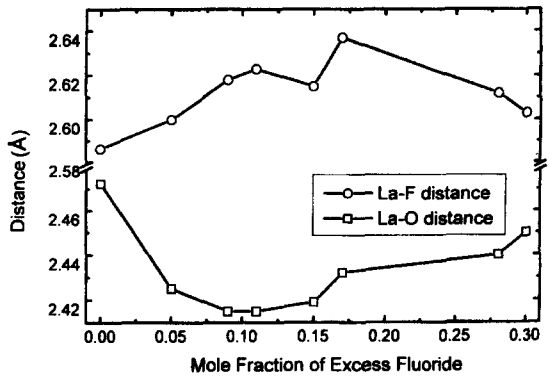


Fig. 4. Evolution of the interatomic Ln—ligand distances in the $LaO_{1-x}F_{1+2x}$ series.

between the two structures lies in the linking of the $OLa_4$ units, which is two-dimensional in the hexagonal and three-dimensional in the tetragonal LaOF. The symmetry of the lanthanum site in the hexagonal LaOF is $C_{3v}$ due to the bicapped trigonal antiprism arrangement of four oxygens and four fluorines. In the tetragonal non-stoichiometric structure, the $La^{3+}$ ion is also eight coordinated to four oxygens and four fluorines but now forming a distorted tetragonal prism with a $C_{4v}$ site symmetry. According to previous luminescence study of the $Eu^{3+}$ doped LaOF and $LaO_{1-x}F_{1+2x}$ [19], the $C_{4v}$ symmetry is well preserved which means that the excess fluorine is not directly coordinated to the lanthanum.

The Ln—ligand distances in the two forms are significantly longer for the non-stoichiometric than for the stoichiometric LaOF and the Ln—F distances are longer than the corresponding Ln—O ones in both phases (Table 2). The evolution of the Ln—F and Ln—O distances in the $LaO_{1-x}F_{1+2x}$ series reveals an interesting detail: for the $x$ value between 0.10 and 0.18 there seems to be a minimum (maximum) for the Ln—O (Ln—F) distances. No such behavior could be observed for the cell parameters. The evolution of the Ln—ligand distances may be due to the changes in the packing of the excess fluorines in the interstitial positions in the fluorine layer.

Table 2. The Ln—O and Ln—F distances in the lanthanum oxyfluoride phases

| Host | Ln—O distance (Å) | Ln—F distance (Å) |
|---|---|---|
| LaOF | 2.408(5)[a] 2.494(23)[b] | 2.578(10)[a] 2.589(26)[b] |
| $LaO_{0.95}F_{1.10}$ | 2.425(4) | 2.600(4) |
| $LaO_{0.91}F_{1.18}$ | 2.415(4) | 2.618(4) |
| $LaO_{0.89}F_{1.22}$ | 2.415(4) | 2.623(4) |
| $LaO_{0.85}F_{1.30}$ | 2.419(4) | 2.615(4) |
| $LaO_{0.83}F_{1.34}$ | 2.432(4) | 2.637(4) |
| $LaO_{0.72}F_{1.56}$ | 2.440(4) | 2.612(4) |
| $LaO_{0.70}F_{1.60}$ | 2.450(4) | 2.603(4) |

[a] Three distances.
[b] One distance.

*Bond valence model calculations*

The bond valence model provides a useful and quantitative description of inorganic bonding in ionic solids [20,21]. In this model, the bond valence calculated from the experimental structural data for each

ion in the structure is compared to the nominal valence. The difference between the bond valence and the nominal valence describes the strains present in the compound. In compounds with bonds of intermediate strength (e.g. the oxides and halides of di- and trivalent cations), the relaxation of the strains can result in the non-stoichiometry, stabilization of unusual oxidation states, distortions in bonding or lowering of the crystal symmetry [22]. With the aid of the bond valence concept, detailed insight to the inherent instability of the compounds, or of the instability of a crystal structure *vis-à-vis* to another polymorph can be obtained for an individual compound [23] or for a series of compounds [24].

The bond valences, $s_{ij}$ for each cation–anion pair can be obtained from the comparison between the experimental interatomic bond distances $R_{ij}$ and the characteristic distance $R_0$ (eq. (1) [12]):

$$s_{ij} = \exp[(R_0 - R_{ij})/B], \quad (1)$$

where $B$ is a universal constant equal to 0.37 [12]. The $R_0$ values can be found in tabulated form for the most frequent cation–anion pairs for oxides and halides [21,25].

The global instability index (GII) value (eq. (2)) derived from the bond valence model can be used to estimate the stability of the structure studied [23]. This quantity is defined by a further comparison between the calculated bond valences $s_{ij}$ and the formal valence $V_i$ for all the species $N$ in the asymmetric unit of the unit cell (eq. (2) [23]):

$$\mathrm{GII} = \sqrt{\sum_{i=1}^{N}\left(\left(\sum_j S_{ij} - V_i\right)^2/N\right)} \quad (2)$$

The global instability index describes also the strains in the structure and put thus a limit to the maximum allowable distortion. According to an empirical formulation, if the GII value exceeds 0.2 the structure becomes unstable and faces a possible collapse or a phase transformation [26].

The global instability index as a function of the $x$ value in $LaO_{1-x}F_{1+2x}$ increases with the increasing excess fluoride indicating diminishing stability with increasing non-stoichiometry. The GII values for all the $LaO_{1-x}F_{1+2x}$ phases are significantly greater than for the stoichiometric LaOF phase, and exceed for most phases the limit of 0.2 for a breakdown of the tetragonal structure. This was effectively shown by the TGA measurements since the thermal decomposition of the non-stoichiometric phases yielded always the stoichiometric LaOF as an intermediate phase. There is no correlation between the $R_{wp}$ and GII values which indicates that the GII value is independent of the quality of the structure solution and is a meaningful quantity appropriate to each structure.

*Factor group analysis*

The factor group analysis was employed to find out the number of the IR and Raman active vibrational modes in the $LaO_{1-x}F_{1+2x}$ system and, subsequently, information on the local structure around the $La^{3+}$ ion. According to the X-ray powder diffraction data presented above, the stoichiometric LaOF belongs to the hexagonal and the non-stoichiometric phases to the tetragonal crystal system.

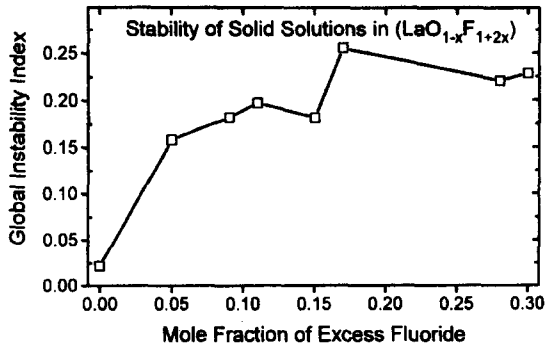


Fig. 5. Evolution of the Global Instability Index (GII) in the $LaO_{1-x}F_{1+2x}$ series.

The theoretical analysis yielded a division of the $3N = 18$ degrees of freedom into 10 modes in the center of the Brillouin zone (with acoustic modes excluded) of the following symmetries:

$$\Gamma_{\mathrm{rhombohedral}} = 3A_{1g} + 2A_{2u} + 3E_g + 2E_u \quad (3)$$

$$\Gamma_{\mathrm{tetragonal}} = A_{1g} + 2B_{1g} + 2A_{2u} + 3E_g + 2E_u \quad (4)$$

According to the group theoretical selection rules [27], the *gerade* modes $3A_{1g}+3E_g$ (rhombohedral) and $A_{1g}+2B_{1g}+3E_g$ (tetragonal) are Raman active whereas the *ungerade* modes $2A_{2u}+2E_u$ (both forms) are IR active.

*FT-IR and FT-Raman spectra*

The results of the factor group analysis were compared to the experimental data. All of the four IR active vibrational modes ($2A_{2u}+2E_u$) for the both forms and five of the six Raman active vibrational modes for the hexagonal ($3A_{1g}+3E_g$) and the tetragonal form ($A_{1g}+2B_{1g}+3E_g$) were observed in the vibrational spectra of LaOF and $LaO_{0.85}F_{1.30}$, respectively (Figs 6 and 7).

The results obtained for the stoichiometric LaOF phase agree well with a previous study [28]. The change in the structure of the lanthanum oxyfluoride was accompanied by significant modifications in both the FT-Raman and FT-IR spectra. The modifications were observed more quantitatively in the FT-Raman (Fig. 7) than in the FT-IR spectra, though there was not much similarity in the latter either (Fig. 6). Moreover, the Raman spectra changed as a function of the excess fluorine since the low frequency vibrations (below 230 $cm^{-1}$) decreased in intensity with increasing excess of fluorine. This might be correlated with the local disorder due to the introduction of the excess fluorine in the interstitial positions in the fluorine

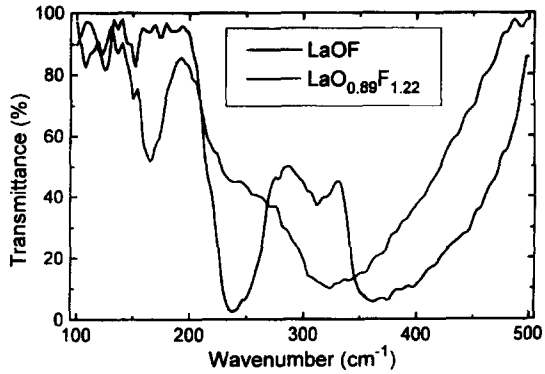


Fig. 6. Comparison of the FT-IR absorption spectra of the stoichiometric LaOF and non-stoichiometric tetragonal $LaO_{0.89}F_{1.22}$ phase.

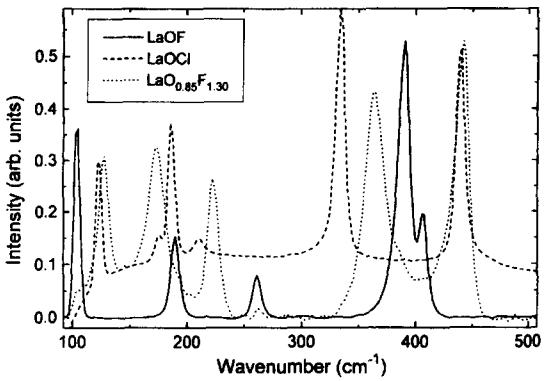


Fig. 7. Comparison of the FT-Raman scattering spectra of tetragonal LaOCl, stoichiometric LaOF and non-stoichiometric tetragonal $LaO_{0.85}F_{1.30}$ phases.

layer. The high energy vibrations seem to be constant irrespective of the fluorine content of the LaOF phase. However, the unambiguous assignment of the vibrations is not possible due to the lack of single crystal data.

Despite the structural isomorphism, the similarity between the Raman spectra of the tetragonal non-stoichiometric $LaO_{1-x}F_{1+2x}$ phase and the tetragonal LaOCl is striking (Fig. 7). The comparison of the spectra facilitated the assignment of some of vibrational modes e.g. the vibrations around 440 and 125 $cm^{-1}$ involve clearly the Ln—O vibrations whereas the other lines originate from vibrations involving the fluorines, too.

## CONCLUSIONS

The stability of the non-stoichiometric $LaO_{1-x}F_{1+2x}$ ($0.05 \leqslant x \leqslant 0.3$) phases was found inferior to the stoichiometric LaOF since the latter phase appeared always during the thermal decomposition. Moreover, global instability index value calculated according to the bond valence model exceeded 0.2 for each $LaO_{1-x}F_{1+2x}$ phase and was significantly greater than that for the stoichiometric LaOF.

All $LaO_{1-x}F_{1+2x}$ phases possess the tetragonal PbFCl-type structure with $P4/nmm$ ($Z = 2$) as the space group. No evidence supporting a symmetry decrease from tetragonal to orthorhombic structure was obtained either from the quality of Rietveld refinements, the splitting or the width of reflections. In agreement with the spectroscopic studies of the $Eu^{3+}$ doped materials no significant distortions of the environment of the lanthanum from tetragonal symmetry was observed from the IR and Raman spectra. The similarity of the Raman spectra to the tetragonal LaOCl confirmed the tetragonal structure of the non-stoichiometric $LaO_{1-x}F_{1+2x}$ phases. The position of the excess fluoride atoms could not be determined but it is evident from the spectroscopic data that they are not coordinated to the host cation.

*Acknowledgements*—Professor Matti Hotokka (Åbo Akademi University) is acknowledged for the use of the FT-Raman equipment. Financial aid from the Finnish Development center for Technology and Ministry of Education (HR) and Academy of Finland (project # 4966) (JH and ES) is acknowledged, too.

## REFERENCES

1. West, A. R., *Solid State Chemistry and Its Applications*, Wiley, Chichester, 1992, pp. 338–340.
2. Smart, L. and Moore, E., *Solid State Chemistry. An Introduction*, 2nd edn., Chapman & Hall, London, 1995, pp. 187–189.
3. Bünzli, J. -C. G., in *Lanthanide Probes in Life, Chemical and Earth Sciences. Theory and Practice*, eds. J. -C. G. Bünzli and G. R. Choppin, Ch. 7, Elsevier, Amsterdam, 1989.
4. Mann, A. W. and Bevan, D. J., *Acta Cryst.*, 1970, **B26,** 2129.
5. Juneja, J. M., Tyagi, A. K., Chattopadhyay, G. and Seetharaman, S., *Mater. Res. Bull.*, 1995, **30,** 1153.
6. Taoudi, A., Laval, J. P. and Frit, B., *Mater. Res. Bull.*, 1994, **29,** 1137.
7. Zachariasen, W. H., *Acta Cryst*, 1951, **4,** 231.
8. Laval, J. P., Abaouz, A., Frit, B., Roult, G. and Harrison, W. T. A., *Eur. J. Solid State Inorg. Chem.*, 1988, **25,** 425.
9. Laval, J. P., Abaouz, A., Frit, B. and Le Bail, A., *Eur. J. Solid State Inorg. Chem.*, 1990, **27,** 545.
10. Blasse, G. and Bril, A., *Solid State Commun.*, 1967, **5,** 1.
11. Young, R. A., ed., *The Rietveld Method*, Oxford University Press, Oxford, 1993.
12. Brown, I. D., *Phys. Chem. Miner.*, 1987, **15,** 30.
13. Hund, F., *Z. Anorg. Allg. Chem.*, 1951, **263,** 52.
14. Hölsä, J. and Niinistö, L., *Thermochim. Acta*, 1980, **37,** 155.
15. Pleskova, I. A., Shakhno, I. V., Plyushchev, V. E. and Sotnikova, M. N., *Inorg. Mater.*, 1971, **7,** 694.
16. Shinn, D. B. and Eick, H. A., *Inorg. Chem.*, 1969, **8,** 232.

17. Sakthivel, A. and Young, R. A., *Program DBWS-9006PC for Rietveld Analysis of X-ray and Neutron Powder Diffraction Patterns*, Georgia Institute of Technology, School of Physics, Atlanta, GA, U.S.A., 1991.
18. Hölsä, J., Kestilä, E., Saez-Puche, R., Dereń, P., Strek, W. and Porcher, P., *J. Phys.: Condens. Mat.*, 1996, **8,** 1575.
19. Hölsä, J., *Acta Chem. Scand.*, 1991, **45,** 583.
20. Brown, I. D. and Altermatt, D., *Acta Cryst., Sect. B*, 1985, **41,** 240.
21. Brown, I. D. and Altermatt, D., *Acta Cryst., Sect. B*, 1985, **41,** 244.
22. Brown, I. D., *Acta Cryst., Sect. B*, 1992, **48,** 553.
23. Brown, I. D., *Z. Krist.*, 1992, **199,** 255.
24. Salinas-Sanchez, A., Garcia-Muñoz, J. L., Rodrigues-Carvajal, J., Saez-Puche, R. and Martinez, J. L., *J. Solid State Chem.*, 1992, **100,** 201.
25. Brese, N. E. and O'Keeffe, M., *Acta Cryst., Sect. B*, 1991, **47,** 192.
26. Armbruster, T., Röthlisberger, F. and Seifert, F., *Am. Mineralog.*, 1990, **75,** 847.
27. Fateley, W. G., Dollish, F. R., McDevitt, N. T. and Bentley, F. F., *Infrared and Raman Selection Rules for Molecular and Lattice Vibrations: The Correlation Method*, Wiley, New York, 1972.
28. Hölsä, J., Pirou, B. and Räsänen, M., *Spectrochim. Acta*, 1993, **49A,** 465.